

We are IntechOpen, the world's leading publisher of Open Access books Built by scientists, for scientists

5,600

Open access books available

137,000

International authors and editors

170M

Downloads

Our authors are among the

154

Countries delivered to

TOP 1%

most cited scientists

12.2%

Contributors from top 500 universities



WEB OF SCIENCE™

Selection of our books indexed in the Book Citation Index
in Web of Science™ Core Collection (BKCI)

Interested in publishing with us?
Contact book.department@intechopen.com

Numbers displayed above are based on latest data collected.
For more information visit www.intechopen.com



Online Estimation of Terminal Airspace Sector Capacity from ATC Workload

Majeed Mohamed

Abstract

Neural Partial Differentiation (NPD) approach is applied to estimate terminal airspace sector capacity in real-time from the ATC (Air Traffic Controller) dynamical neural model with permissible safe separation and affordable workload. A neural model of a multi-input-single-output (MISO) ATC dynamical system is primarily established and used to estimate parameters from the experimental data using NPD. Since the relative standard deviations of these estimated parameters are lesser, the predicted neural model response is well matched with the intervention of ATC workload. Moreover, the proposed neural network-based approach works well with the experimental data online as it does not require the initial values of model parameters that are unknown in practice.

Keywords: ATC (Air Traffic Controller) workload, terminal airspace capacity, estimation and dynamic modeling, neural partial differentiation, output error method

1. Introduction

Accurate estimation of the air traffic capacity is a pillar of efficient air traffic management, which provide efficient use of airspace resources and controlling resources to meet the air traffic demand [1]. Suppose trajectories of all flights and the capacity of all resources are known with certainty for some planning horizon. In that case, there exist computationally feasible approaches to managing the traffic that minimizes overall delay cost [2–6]. But the uncertainty makes traffic flow management difficult. At any given time, the weather is the driving force in determining the number of flights in the airport or sector in the aspect of capacity. Air traffic controllers (ATC) confirm airspace's safe operation by ensuring all aircraft under their authority maintain safe separation with the assistance of technology and international rules and regulations [7]. The role of ATC is becoming more crucial as air traffic growth increases. So traffic growth will introduce more aircraft operations in the busy ATC sectors with high air traffic density. The significant effect of such an increase in air traffic has been the rise in flight delays in the region. As a result, an economic impact of flight delays is included in the safe operation of airspace. Individual aircraft delay is increased whenever air traffic demand nears capacity. Therefore, unacceptable delays result from exceeding progressive hourly traffic demands to the hourly capacity of the air traffic. The aircraft delays will not

decrease even if the hourly demand is less than the hourly capacity for the demand within a portion of the time interval that exceeds the capacity during that interval.

In the en-route environment, the airspace is segmented into air traffic control ATC sectors, the geographical volume of airspace. By keeping safety as a priority in operation, the capacity of an ATC sector can be defined as the maximum number of aircraft that are controlled in a particular ATC sector in a specified period while still permitting an acceptable level of controller workload. For more clarity, we need to realize i) What is meant by the controller workload? ii) How is this controller workload measured? iii) What is the acceptable level of controller workload? i.e. the threshold value at capacity. Thus, the workload is a process or experience that cannot be seen directly but must be understood from what can be seen or measured. In the present scenario of air transport, air traffic is increasing rapidly and becomes airspace congestion. Airspace capacity needs to be increased to address the airspace congestion problem. Since the airspace sector capacity is determined mainly by controller workload, a typical air transport schematic is given in **Figure 1**, highlighting the controller workload problem [8, 9]. Controller workload is the effort expended by the controller to manage air traffic events. It refers to the physical and mental effort an individual exerts to perform a task. A measure of the ATC Workload is required to evaluate the effects of new systems and the procedures on individual air traffic controllers.

Certain airspace capacity issues can be addressed by minimizing the controller overload and clarifying the necessity of understanding and modeling the controller workload. The critical factors affecting controller workload are sector, and air traffic characteristics [8, 9] and those factors are given in **Figure 2**. The factors affecting air traffic and sectors are listed in **Table 1** [10]. Measurement of controller workload can be achieved from the information on the i) communication between the ATC officer and the pilot and ii) communication between the ATC officers of adjacent sectors. The number of aircraft movements per hour, number of heading changes, number of altitudes changes and number of speed changes are the information on monitoring workload. Various methods are discussed in the literature for measuring the workload of air traffic controllers [11, 12]. They are self-assessment [13, 14] and direct observations of the controllers by other controllers or ATC system experts. Moreover, the workload experienced by air traffic controllers is affected by the complex integration of: 1) the air traffic and the sector in the airspace, 2) the accuracy of equipment in the control room and in the aircraft, and 3) the controller's

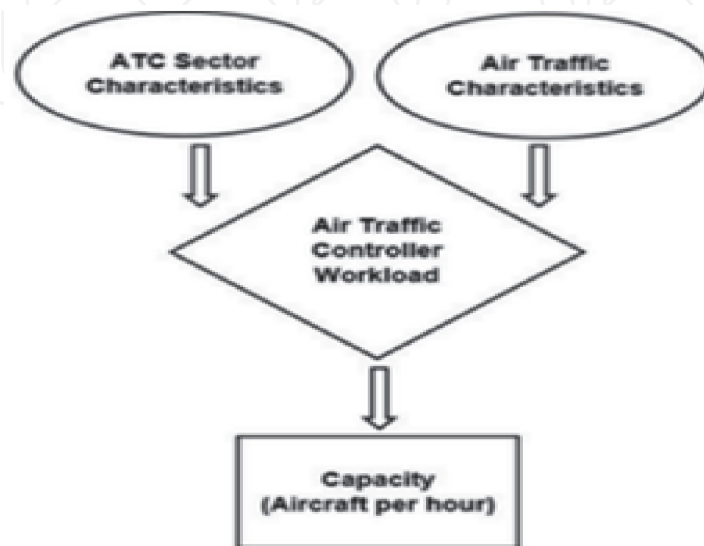


Figure 1.
Air transport schematic with controller workload.

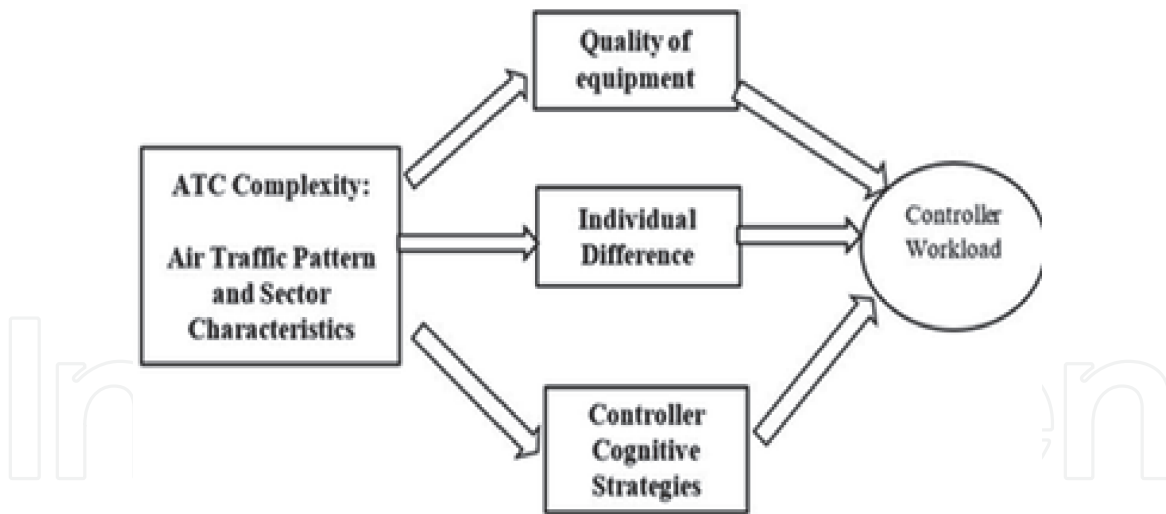


Figure 2.
 Controller workload factors.

| Sr. No | Factors affecting air traffic | Factors affecting sectors |
|--------|-----------------------------------|-------------------------------------|
| 1 | Total number of aircraft | Sector size |
| 2 | Peak hourly count | Sector shape |
| 3 | Traffic Mix | Boundary location |
| 4 | Climbing / Descending aircraft | Number of intersection points |
| 5 | Aircraft speeds | Number of flight levels |
| 6 | Horizontal separation standards | Number of facilities |
| 7 | Vertical separation standards | Number of entry and exit points |
| 8 | Average flight duration in sector | Airway Configuration |
| 9 | Total flight time in sector | Proportion of unidirectional routes |
| 10 | Average flight direction | Number of surrounding sectors |

Table 1.
 Factors affecting air traffic and sector.

age, experience, decision-making strategies. Another possible approach to measuring ATC workload is to form a functional relationship between the controller workload and the associated model parameters. To achieve that relationship, we must vary several possible airspace and traffic parameters systematically in simulation modeling of airspace and controller workload [15].

The ideal approach to estimate airspace capacity is to build an accurate capacity model from the direct observation of the controller's workload using a system identification procedure. The derived statistical model will represent the actual capacity of sectors and airspace under alternative controller working processes [8]. To validate such a model, one needs to collect the data for a sufficient period and over a range of different individual controllers. Many difficulties need to address the collection of field data at each ATC sector. Observing controllers at work as unobtrusively as possible is not an easy task. Moreover, more resources are also required to transcribe the data from videotape, communications tapes, and flight strips. As a result, vast resources and complex logistics are needed for this approach precluded for this research. The construction of an operational environment using real-time simulations is an alternative method with the technology to be tested and pseudo-pilots. Such real-time simulation provides the human workload and traffic

handling capacity, which are very costly exercises posing many problems in personnel training, infrastructure, and obtaining a high-fidelity simulation of the operating environment [16]. These disadvantages rule out a real-time simulation for this research.

In short, the en-route sector capacity is determined mainly by controller workload [9, 17]. A method has been derived to estimate sector capacity from the controller's workload and translate that into a capacity measure [17–19]. In bright weather situations, the capacity of a sector is represented by the Monitor Alert Parameter, which is roughly 5/3 times the average historical dwell time for flights in that sector [20]. En-route capacity estimation from ATC workload becomes a more difficult task when hazardous weather increases the intensity of all workload types [21–23]. The main contributions of this chapter are

- Terminal airspace sector capacity is estimated from experimental data along with the derivation of ATC dynamical model. Neural partial differentiation (NPD) and output error method (OEM) are used for this purpose, and their results are compared. An appropriate probability density function (pdf) of 'Time interval X' is derived and analytically verified for the accurate modeling of ATC dynamic system.
- Since the uncertainty in traffic flow and dependency of weather conditions make the data to stochastic, the proposed neural network-based approach works well with the experimental data in online as it can handle the noisy data without knowing the noise covariance matrix and does not require the initial values of the model parameters which are unknown in practice. As a result, a three-dimensional capacity curve has been established using the estimates of NPD to predict the air traffic capacity in real-time.

The chapter is organized as follows: Section 2 discusses mathematical model postulates for the estimation of Terminal Airspace Capacity with analysis of flight data. Moreover, dynamic modeling of ATC with estimation of model parameters using neural partial differentiation (NPD) are described in the following subsections of section 2. The online estimation result of airspace capacity is presented in Section 3, and finally, the conclusions are given in Section 4.

2. Estimation of terminal airspace sector capacity

2.1 Problem definition

The estimation of airspace sector capacity $C_s(k)$ in (Eq.(1)) can be viewed as dynamic modeling of ATC by estimating the parameter θ at which variables x_1, x_2, x_3 are satisfying the following inequality relation (Eq.(2)) with maximum affordable value of ATC workload represented in terms of $G(\cdot)$;

$$C_s(k) = x_1(k) + x_2(k) + x_3(k) \quad (1)$$

$$f(x_1(k), x_2(k), x_3(k), \theta) \leq G(h(X(k))), k = 1, 2, 3, \dots, N \quad (2)$$

where $f(x_1, x_2, x_3, \theta)$ represents the dynamical model of ATC, θ is the vector of model parameters, x_1 is total number of departing aircraft during an unit time, x_2 is total number of arriving aircraft during an unit time, x_3 is total number of flyover aircraft during an unit time, $G(\cdot)$ is number of control events (messages between pilot and ATC) that occurred in unit time, $h(X)$ is function associated

with the workload of ATC, and X is interval time of the consecutive events (messages) in sec.

2.2 Flight data analysis

The recorded flight data of the third sector of Kunming TMA at Kunming airport, China is analyzed to estimate the terminal airspace sector capacity from the ATC workload [24]. Terminal Maneuvering Area (TMA) is designated area of controlled airspace surrounding a significant airport where there is a high volume of traffic. This data is based on the workload of ATC during the entire day; it consists of voice communication (messages) between ATC officers and pilots or adjacent sectors. These messages are referred to control events exhibit intermittency, i.e., they occur in several time frames with “short interval and high frequency” or vice versa based on the traffic congestion. For the definition of a function $h(X)$ in (Eq.(2)), the field data of air traffic can be gathered from the ATC officers at the Kunming airport using voice recording equipment of the air traffic control department. The time interval of the 1000 consecutive events on 21st January 2014, is recorded in the third sector of Kunming TMA, which is given in **Figure 3** [24].

Data statistics are made with MATLAB and found the histogram of time interval X to derive the density distribution function $P(X)$ in **Figure 4**. This indicates that experimental data show power-law distribution whose probability density function is given by.

$$P(X) = CX^{-\alpha} \quad (3)$$

The distribution characteristics of power-law function can be verified by a theoretical method; the parameter C and α are computed by the following maximum likelihood estimation (MLE) approach. By taking the logarithm of (Eq.(3)), we have.

$$\log(P(X)) = \log(C) - \alpha \log(X) \quad (4)$$

The relationship represents a straight line with a gradient of $-\alpha$ in the double logarithmic coordinates. The normalization equation is.

$$1 = \int_{X_{\min}}^{\infty} P(X)dX = C \int_{X_{\min}}^{\infty} X^{-\alpha}dX \Rightarrow C = (\alpha - 1)X_{\min}^{\alpha-1}, \alpha > 1 \quad (5)$$

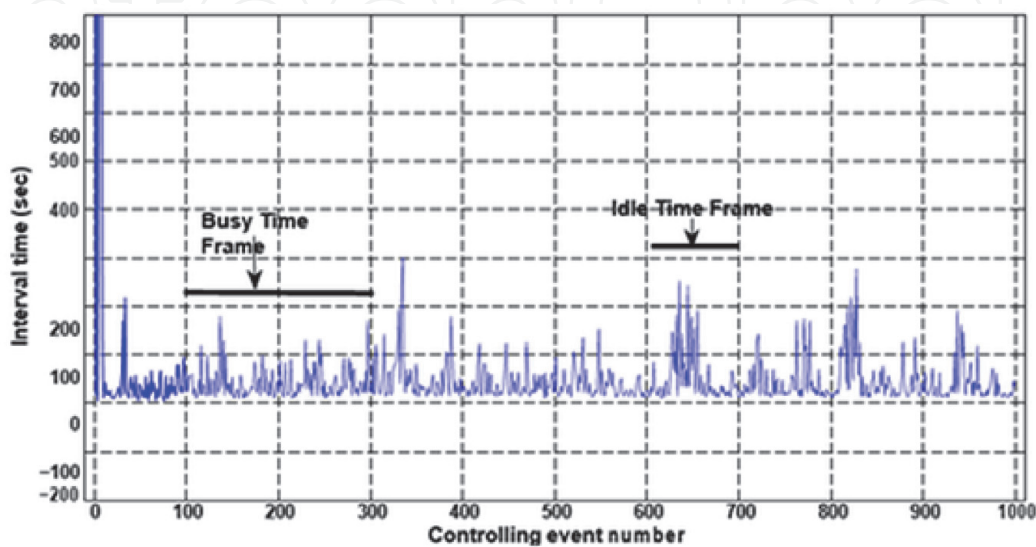


Figure 3.
 Interval time of ATC.

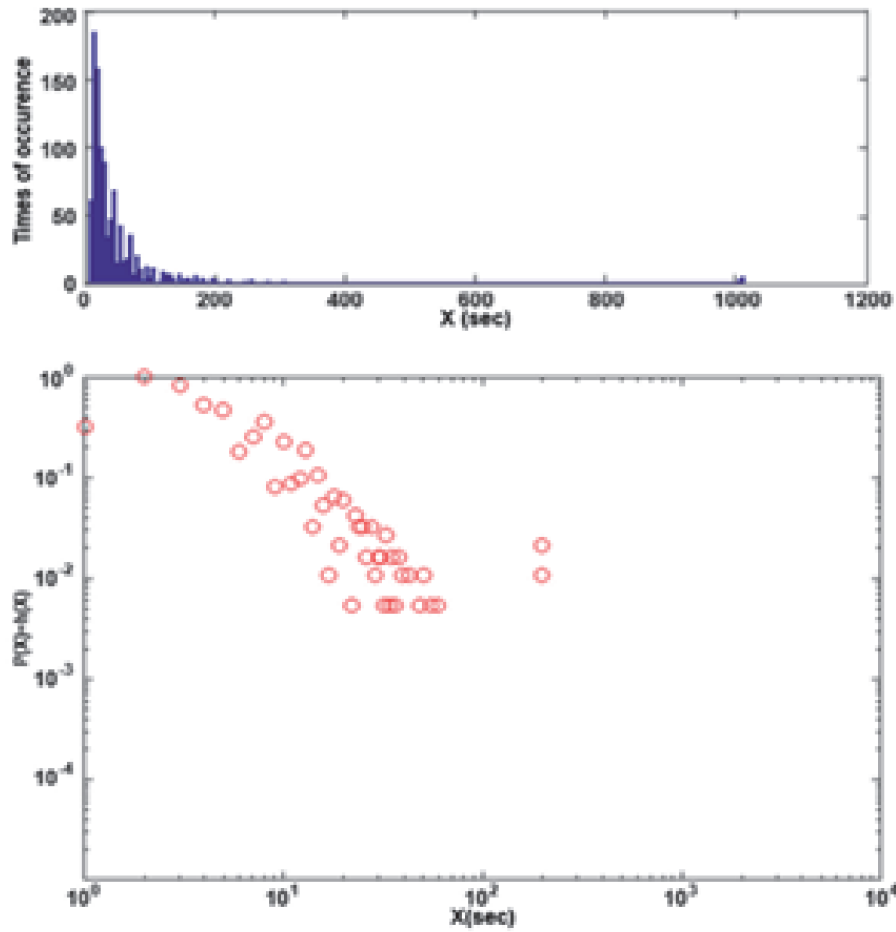


Figure 4.
Density distribution of Time Interval.

Where X_{min} is the minimum possible value of X . The power law distribution is

$$P(X) = \frac{(\alpha - 1)}{X_{min}} \left(\frac{X}{X_{min}} \right)^{-\alpha} \quad (6)$$

For a given set X_i , probability of X_i is

$$Pr.(X/\alpha) = \prod_{i=1}^N \frac{(\alpha - 1)}{X_{min}} \left(\frac{X_i}{X_{min}} \right)^{-\alpha} \quad (7)$$

For convenience, the logarithm of Maximum Likelihood Function L is given by

$$L = \ln Pr.(X/\alpha) = \sum_{i=1}^n \left[\ln(\alpha - 1) - \ln X_{min} - \alpha \ln \frac{X_i}{X_{min}} \right] \quad (8)$$

$$\frac{\partial L}{\partial \alpha} = 0 \Rightarrow \alpha = 1 + n \left[\sum_{i=1}^n \ln \frac{X_i}{X_{min}} \right]^{-1} = 2.25, C = 122.36$$

Thus, probability density function of power law distribution becomes.

$$P(X) = 122.36X^{-2.25} \quad (9)$$

We found that the experimental data agree with the distribution characteristic of power-law function by theoretical computation of (Eq.(9)) as shown in **Figure 5**.

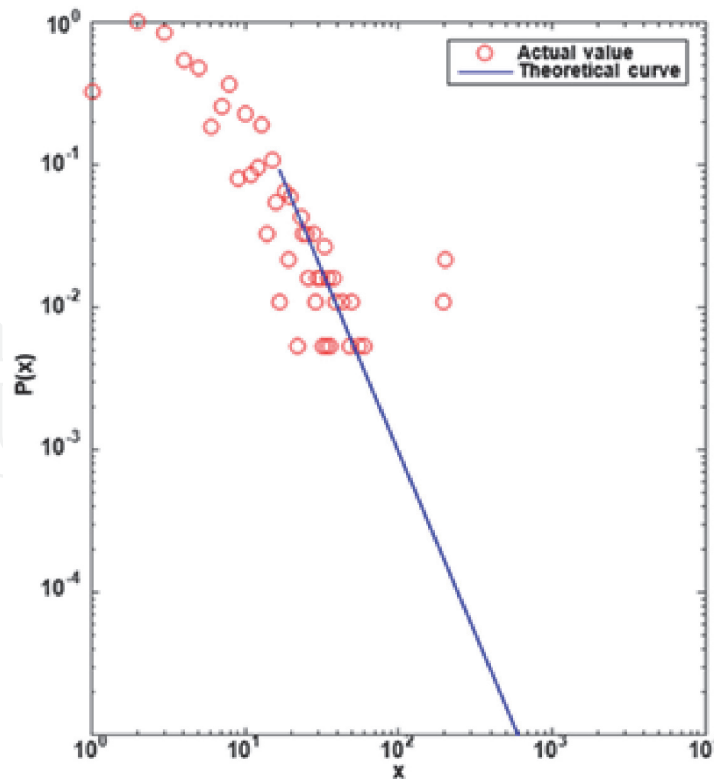


Figure 5.
 Density distribution of Time Interval.

The R^2 value of the data fitting is observed to be 0.83. Now the left side of expression $G(h(X))$ in (Eq.(2)) can be computed with the threshold criterion of 80 percent. Since the sector capacity is expressed in terms of a number of control events that occurred within one hour of the estimation time, the reasonable controlling workload time should be $2880 (= 3600 * 80/100)$ seconds. Subsequently, sector capacity is estimated by representing $G(h(X))$ is the number of control events that occurred within one hour as follows.

$$G(.) = \frac{2880}{E(X)} \quad (10)$$

where $E(X)$ is average interval time (X) of the consecutive events in sec, and it is given by

$$E(X) = \left(\frac{C}{\alpha - 1} \right)^{\frac{1}{\alpha - 1}} \left(\frac{\alpha - 2}{\alpha - 1} \right), \alpha > 2 \quad (11)$$

Next, to estimate the airspace sector capacity, we need to build the dynamical model of ATC and estimate the model parameters.

2.3 ATC dynamic modeling and parameter estimation

2.3.1 Neural dynamic modeling of ATC

Based on the equality relation of (Eq.(1)), the dynamical model of ATC represented by $f(x_1, x_2, x_3, \theta)$ can be modeled using Neural Networks [25]. **Figure 6** shows the three-layered feed-forward neural network's schematic structure, which consists of two hidden layers with activation function and one output layer with

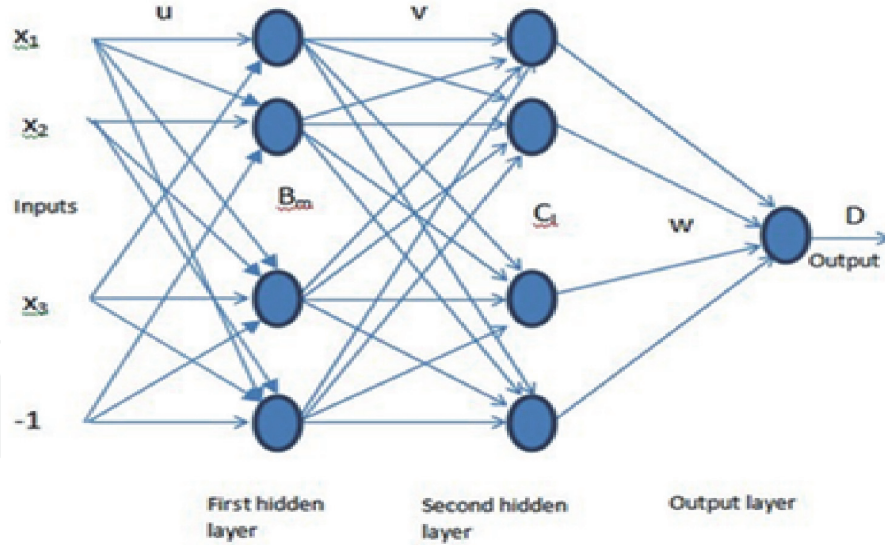


Figure 6.
Schematic of neural network.

summation function exempted from activation function. An approach of back-propagation trains the neural network whose input and output vectors are defined by $x = [x_1, x_2, x_3, -1]$ and $D = G$ respectively. Similarly, $B \in \mathfrak{R}^{m+1}$ and $C \in \mathfrak{R}^{l+1}$ represents the first and second hidden layer of neural network. Except for the output layer, all the layers contain a bias term, and the output of the neural network is given by.

$$G = W^T C \quad (12)$$

where W is the set of weights between the second hidden layer and output layer containing the bias terms.

$$W = [b_{w1} \quad w_{11} \quad \cdots \quad w_{l1}]^T \quad (13)$$

Similarly we define

$$\begin{cases} C = q(V^T B) \\ B = g(U^T x) \end{cases} \quad (14)$$

where q and g are the activation function vectors and are defined as $[-1 \ q(x_1)]^T$, where $q(x)$ is expressed as

$$q(x) = \frac{1 - e^{-\lambda x}}{1 + e^{-\lambda x}} \quad (15)$$

And the weight matrix are represented as

$$[V] = \begin{bmatrix} b_{v1} & \cdots & b_{vm} \\ v_{11} & \cdots & v_{1l} \\ \cdots & \cdots & \cdots \\ v_{m1} & \cdots & v_{ml} \end{bmatrix} \quad (16)$$

$$[U] = \begin{bmatrix} b_{u1} & \dots & b_{um} \\ u_{11} & \dots & u_{1m} \\ u_{21} & \dots & u_{2m} \\ u_{31} & \dots & u_{3m} \end{bmatrix} \quad (17)$$

Input is defined by the vector $x = [x_0, x_1, x_2, x_3]$, where x_0 defines bias input to the neural network. The input and output are scaled for neural network using the following equation.

$$G_{i,norm} = G_{i,norm_{min}} + (G_{i,norm_{max}} - G_{i,norm_{min}}) \times \left(\frac{G_i - G_{i,min}}{G_{i,max} - G_{i,min}} \right) \quad (18)$$

where $G_{i,norm_{max}}$ and $G_{i,norm_{min}}$ denote the higher and lower limits of scaling range of G_i respectively. They are set to 0.9 and -0.9 respectively. $G_{i,max}$ and $G_{i,min}$ denote the higher and lower values of G_i . Using the above notations, output of neural network can be written as.

$$G = W^T q [V^T g(U^T x)] \quad (19)$$

2.3.2 Parameter estimation using neural partial differentiation method

The neural network is trained with input and output data to map the functional relationship of (Eq.(1)) in the form of weights, and its activation function operates the core of the neural partial differentiation method as parameter estimation approach. The constant parameters of air traffic model can be directly computed from the end of the training session of a neural network by the partial differentiation of a function, and it is as follows.

The input and output of a function is mapped after the training session of the neural network. Subsequently, the output variables can be differentiated with respect to input variables. Differentiate (Eq.(12)) and (Eq.(14)), we will have the form of.

$$\frac{\partial G}{\partial C} = W^T \quad (20)$$

$$\frac{\partial C}{\partial B} = q'(V^T) \quad (21)$$

$$\frac{\partial B}{\partial x} = g'(U^T) \quad (22)$$

Multiplication of (Eq.(20)), (Eq.(21)), and (Eq.(22)) gives.

$$\begin{cases} \frac{\partial G}{\partial C} \cdot \frac{\partial C}{\partial B} \cdot \frac{\partial B}{\partial x} = W^T \cdot q' V^T \cdot g' U^T \\ \frac{\partial G}{\partial x} = W^T \cdot q' V^T \cdot g' U^T \end{cases} \quad (23)$$

where $q' = \text{diag}[0 \ q'_1 \ \dots \ q'_l]$ and $g' = \text{diag}[0 \ g'_1 \ \dots \ g'_m]$. If the input and output of neural network are normalized, then

$$\frac{\partial G}{\partial x} = \frac{\partial G}{\partial G_{norm}} \times \frac{\partial G_{norm}}{\partial x_{norm}} \times \frac{\partial x_{norm}}{\partial x} \quad (24)$$

The normalized output of neural network can be de-normalized by (Eq.(18)). Where,

$$\left[\frac{\partial x_{norm}}{\partial x} \right] = \begin{bmatrix} 1 & 0 & 0 & 0 \\ 0 & \frac{\partial x_{1,norm}}{\partial x_1} & 0 & 0 \\ 0 & 0 & \frac{\partial x_{2,norm}}{\partial x_2} & 0 \\ 0 & 0 & 0 & \frac{\partial x_{3,norm}}{\partial x_3} \end{bmatrix} \quad (25)$$

The equation (Eq.(25)) can be computed from (Eq.(18)). The terms associated of (Eq.(20)) to (Eq.(25)) be intermediate terms of neural networks while getting it trained. Therefore, there is no extra computation required to compute the parameters, and they are directly given as:

$$\left\{ \frac{\partial G}{\partial x} \right\} = \left[\frac{\partial G}{\partial x_0} \quad \frac{\partial G}{\partial x_1} \quad \frac{\partial G}{\partial x_2} \quad \frac{\partial G}{\partial x_3} \right] \quad (26)$$

The standard deviation of estimated parameters in (Eq.(26)) is computed by

$$S_{TD} = \sqrt{\frac{\sum_{p=1}^P \left[\sum_{m=1}^M \left(\sum_{l=1}^L C'_{lp} v_{lm} w_{kl} G'_{k_p} \right) B'_{m_p} u_{mi} - \mu \right]^2}{P}} \quad (27)$$

where,

$$\mu = \frac{\sum_{p=1}^P \sum_{m=1}^M \left(\sum_{l=1}^L C'_{lp} v_{lm} w_{kl} G'_{k_p} \right) B'_{m_p} u_{mi}}{P} \quad (28)$$

where, S_{TD} and μ are standard deviation and average of data points, respectively. The relative standard deviation of estimates is given by

$$R_{STD} = \frac{S_{TD}}{\mu} \times 100\% \quad (29)$$

3. Online estimation results and discussion

As a part of ATC dynamic modeling, online estimation of the model parameters from flight data is carried out using Neural partial differentiation (NPD) method [26], and estimates are compared with that obtained by Maximum likelihood estimation (Output Error Method). The model structure of the dynamical ATC is given by [27].

$$y = x_1\beta_1 + x_2\beta_2 + x_3\beta_3 + e \quad (30)$$

where y is the number of control events that occurred in unit time, which represents an ATC workload, x_1 is the total number of arriving aircraft during a unit time, x_2 is the total number of departing aircraft during a unit time, x_3 is the total number of flyover aircraft during a unit time. ATC model parameters $\beta_1, \beta_2, \beta_3$ in (Eq.(30)) are coefficient terms which are needed to be estimated for a given set of y and x_1, x_2, x_3 values, and e is a random error term represents model uncertainty. A

neural model of ATC has been established by training of the input–output flight data. An approach of Neural Partial Differentiation (NPD) can be applied to extract the model parameters $\beta_1, \beta_2, \beta_3$. From the neural model of ATC, and their corresponding standard and relative standard deviations can compute using (Eq.(27)) and (Eq.(29)). **Figure 7** shows responses of the input signals (x_1, x_2, x_3) to the neural network and the output signal of workload y , represent the number of control events in a unit time. The dotted red color line indicates the output of trained neural network as estimated output, which reasonably matches with measured data of workload. **Figure 8** shows the estimated model parameter using the NPD method concerning the different data points. The variation of these parameters for the number of iterations is shown in **Figure 9**. As the number of iterations increases, the parameters attain a stable value of its estimates.

Unlike the OEM approach, initial values of model parameters are not needed in the application of NPD method, but it requires apriori structure of the model. The initial values of parameters are chosen as $\beta_1(0) = 0.0001, \beta_2(0) = 0.0001, \beta_3(0) = 0.0001$ for the application of output error method (OEM) in comparison. The responses of measured data of workload concerning control events and its estimated responses using OEM are given in **Figure 10**. and found that they are in close agreement with others. The results of the estimated parameters are tabulated in **Table 2**. The relative standard deviation of estimated parameters is computed in percentage and separately given in parenthesis. These values denote the confidence level of the corresponding estimate. It can be observed from **Table 2** that Neural Partial Differentiation (NPD) approach estimated parameters with less relative standard deviation compared to the output error method (OEM). As a result, estimated parameters of ATC dynamic model using NPD are more accurate in comparison with the Maximum likelihood (OEM) estimates.

The estimated ATC model is verified by the model validation as it is the last process in the model building procedure. For this, the complementary data set of input and output (other than the data used for the training of neural network) are used to predict the neural model of ATC. **Figure 11** shows how the measured response of workload compared with a predicted neural model of ATC and the estimated model by OEM. The validation of the model showed that match between the complement data response and predicted neural model response is good

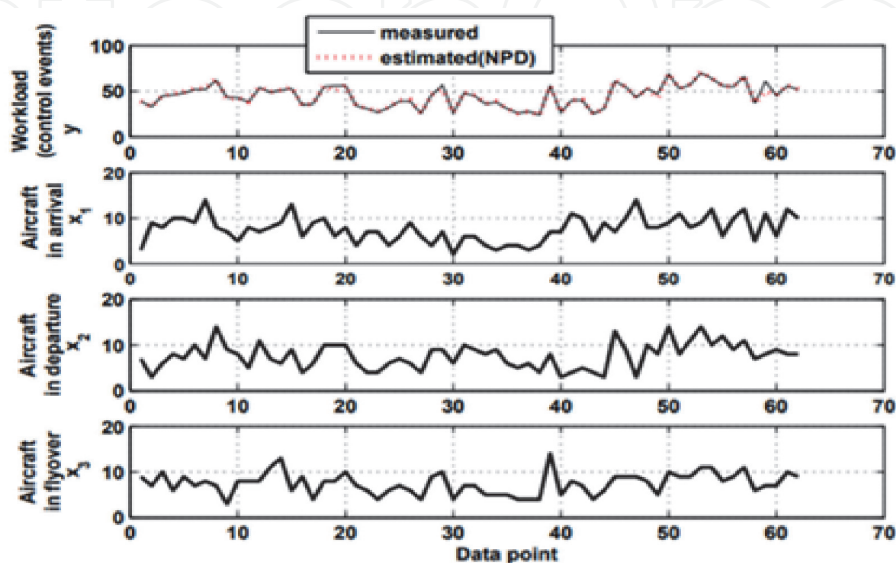


Figure 7.
 Responses of measured data and neural dynamical model of ATC.

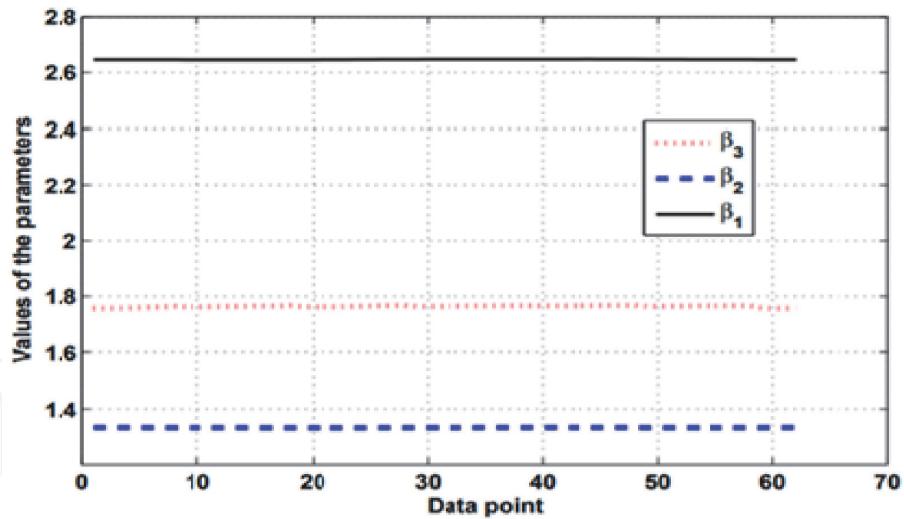


Figure 8.
Variation in estimated parameters with respect to data points using NPD.

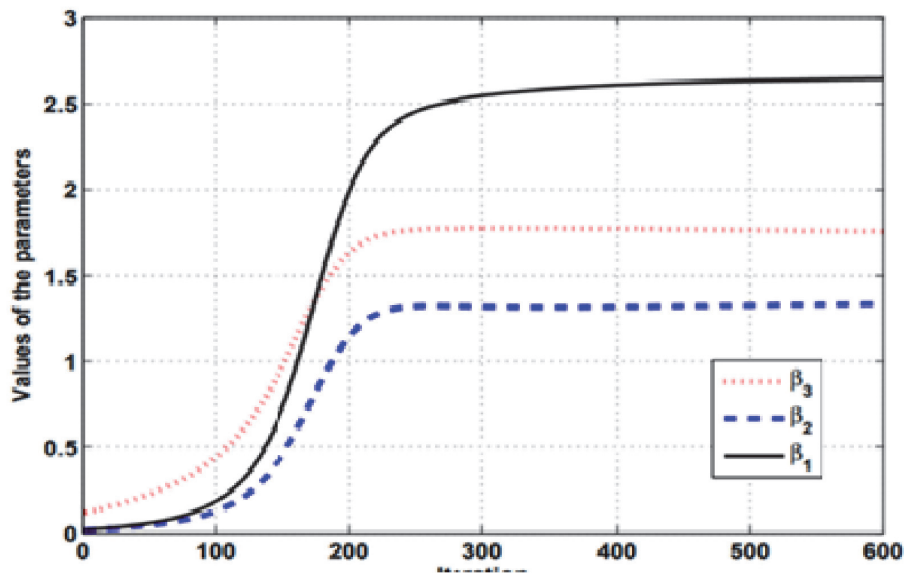


Figure 9.
Variation in estimated parameters w.r.t. number of iterations using NPD.

agreement compared to the response of OEM estimated model. Such compared result reconfirms that parameter estimates by NPD are closer to the actual values. Finally, this ensures that the dynamic model of ATC has been accurately identified. Subsequently, we can use (Eq.(10)) and correctly estimated ATC model to predict the capacity of a sector by reducing the inequality relation (Eq.(2)) into.

$$2.652x_1(k) + 1.339x_2(k) + 1.744x_3(k) \leq \frac{2880}{E(X)}, k = 1, 2, 3, \dots, N \quad (31)$$

Based on the analysis of Kunming TMA data with computation of average time interval $E(X) = 47.21$ with $\sigma = 2.25$, an upper bound of ATC workload of $(2880/47.21) \approx 61$ can be computed for applying to the inequality relation (Eq. (31)). **Figure 12** shows the numerical simulation result of that relationship as a capacity curve to predict the air traffic capacity. Based on the number of flyover aircraft x_3 , either possible cases of the number of arriving aircraft x_1 or the number of departing aircraft x_2 can be adjusted according to within the capacity curve. As a

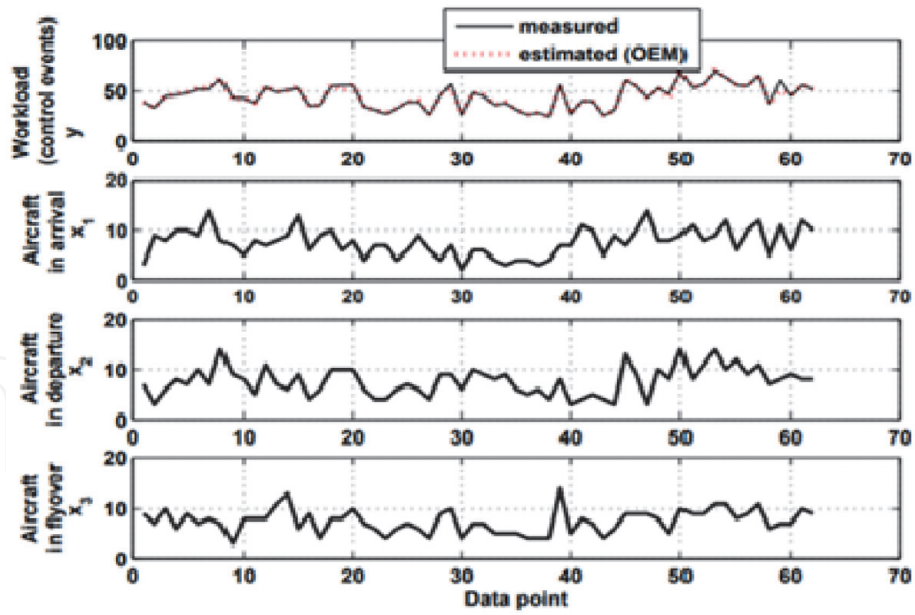


Figure 10.
 Responses of measured and estimated workload using OEM.

| Parameters | NPD | OEM |
|------------|----------------------------|---------------|
| β_1 | 2.652 (2.52 ¹) | 2.8939 (2.90) |
| β_2 | 1.339 (2.405) | 1.4634 (5.87) |
| β_3 | 1.744 (1.659) | 1.5799 (7.16) |

¹The values in parenthesis denote relative standard deviation values in percentage.

Table 2.
 Analysis of estimated parameters.

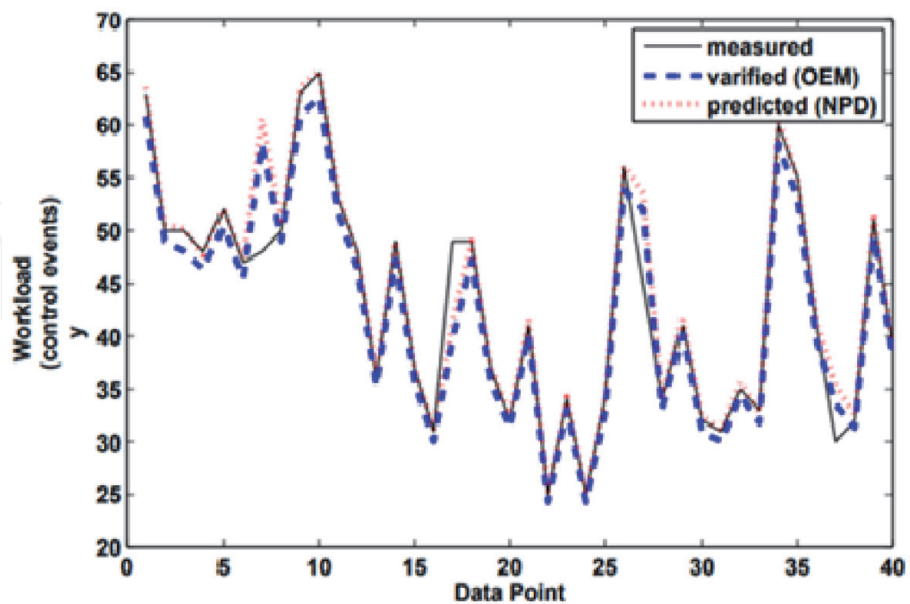


Figure 11.
 Validation of estimated dynamic model of ATC.

result, air traffic capacity can be directly predicted from three-dimensional **Figure 12**. For a wide range of operation varies from less to more traffic congestion scenario with multi-dimensional tasks, postulated linear model might not be

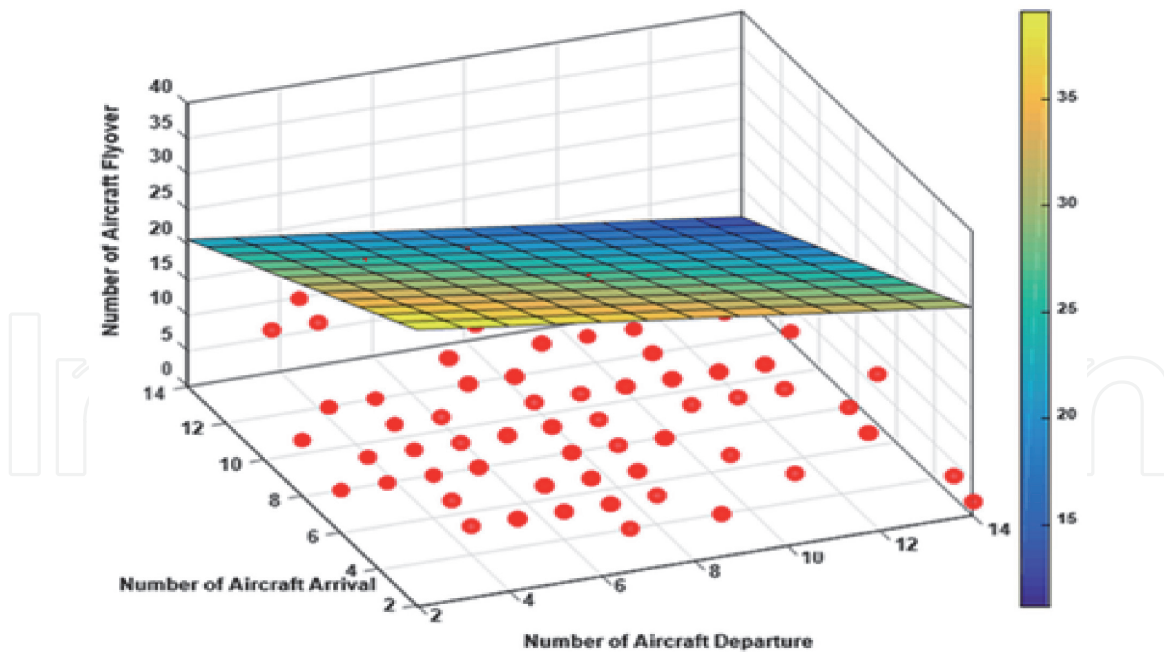


Figure 12.
Capacity curve.

sufficient to obtain a valid model of ATC. In such a case, research work on a nonlinear model of ATC can be considered as future work.

4. Conclusions

ATC dynamical model-based airspace sector capacity has been estimated. The Neural Partial Differentiation (NPD) and Output Error Method (OEM) are used as parameter estimation methods for this purpose. Neural Partial Differentiation (NPD) approach is applied to recorded data of the third sector of Kunming TMA to estimate the ATC dynamic model parameters. For this purpose, a primarily neural model of multi-input- single-output (MISO) ATC system is established. NPD method is employed to extract the model parameters from the experimental data, and the estimated parameters are compared with estimates obtained from the Output Error Method. We found that estimated parameters by NPD are much closer to the actual values compared to the estimates by OEM. This is because of 1) estimated parameters by NPD are having less relative standard deviation and 2) model validation results show that predicted neural model response is well matched with the response for the compliment dataset of ATC workload. Since the initial values of parameters are not available in a practical situation as well as OEM requires these initial parameters, the neural network approach works well with the experimental data. Finally, terminal airspace sector capacity curve has been developed to predict the air traffic capacity with permissible separation and affordable workload.

Acknowledgements

The author is grateful to thank Dr. Su Rong, faculty at NTU, Singapore, for carrying out this research work at Air Traffic Management Research Institute in Singapore.

Nomenclature

| | |
|--------------------------------------|--|
| x_1 | Total number of departing aircraft during an unit time |
| x_2 | Total number of arriving aircraft during an unit time |
| x_3 | Total number of flyover aircraft during an unit time |
| $\theta = \beta_1, \beta_2, \beta_3$ | ATC model parameters |
| $G(\cdot)$ | Number of control events |
| e | Random error due to model uncertainty |
| STD | Standard deviation of data points |
| μ | Average of data points |
| R_{STD} | Relative standard deviation of estimates |

Abbreviations

| | |
|------|--------------------------------|
| NPD | Neural Partial Differentiation |
| ATC | Air Traffic Controller |
| MISO | Multi Input Single Output |
| OEM | Output Error Method |
| TMA | Terminal Maneuvering Area |
| MLE | Maximum Likelihood Estimates |

Appendix A: Output error method

In the output error method (OEM), the unknown parameters are obtained by minimization the sum of weighted square differences between the measured outputs and model outputs. The estimation problem is non-linear because of unknown parameter appears in the aircraft equations of motion and they are integrated to compute the states. Outputs are computed from states, control input and parameters using the measurement equation. Iterative nonlinear optimization techniques are required to solve this nonlinear estimation problem [28–30].

The mathematical model aircraft is assumed to be describe following general linear dynamics system representation.

$$\begin{aligned} \dot{x}(t) &= Ax(t) + Bu(t), x(t_0) = x_0 \\ y(t) &= Cx(t) + Du(t) \\ z(t_k) &= y(t_k) + v(t_k), k = 1, 2, 3, \dots N \end{aligned} \quad (32)$$

where x is the $(n_x + 1)$ state variables, u the $(n_u + 1)$ control input vector, y the $(n_z + 1)$ system output vector, and measurement vector z is sampled at N discrete points. The Matrices A, B, C and D contain the unknown system parameters and are given by

$$\Theta = [(A_{ij}, i = 1 \text{ to } n_x; j = 1 \text{ to } n_x)^T (B_{ij}, i = 1 \text{ to } n_x; j = 1 \text{ to } n_x)^T (C_{ij}, i = 1 \text{ to } n_y; j = 1, n_x)^T (D_{ij}, i = 1 \text{ to } n_y; j = 1 \text{ to } n_u)]^T \quad (33)$$

In order to estimate the likelihood function to estimate the parameter of dynamic system represented in (Eq.(32)), the following assumption:

- The exogenous input sequence $[u(t_k), k = 1, 2, 3 \dots N]$ is independent of the system output.

- The measurement errors $[v(t_k) = z(t_k) - y(t_k)]$ at different discrete points are statically independent, the assume to be distributed with zero means and covariance matrix R , that is, $E[v(t_k)] = 0, E[v(t_k)v^T(t_l)] = R\delta_{kl}$
- The system is corrupted by measurement noise only.
- Control input $u(t_k)$ are sufficiently and adequately (i.e. in magnitude and frequency) varied to excite directly or indirectly the various modes of the dynamics system being analyzed.

The maximum likelihood output error estimates of unknown parameters are obtained by minimizing the negative logarithm of the likelihood function. **Figure 13** shows a block schematic of the output error method (OEM). The cost function of this method is considered in (Eq.(34)).

$$J(\Theta) = \frac{1}{2} \sum_{k=1}^N [z(t_k) - y(t_k)]^T R^{-1} [z(t_k) - y(t_k)] + \frac{N}{2} \ln |R| \quad (34)$$

Where is covariances matrix of the residuals and estimates can obtain from the (Eq.(35)). When started from suitably specified initial value, the estimates are iteratively updated using Gauss-Newton method.

$$R = \frac{1}{N} \sum_{k=1}^N [z(t_k) - y(t_k)]^T [z(t_k) - y(t_k)] \quad (35)$$

The algorithmic steps of OEM are given below.

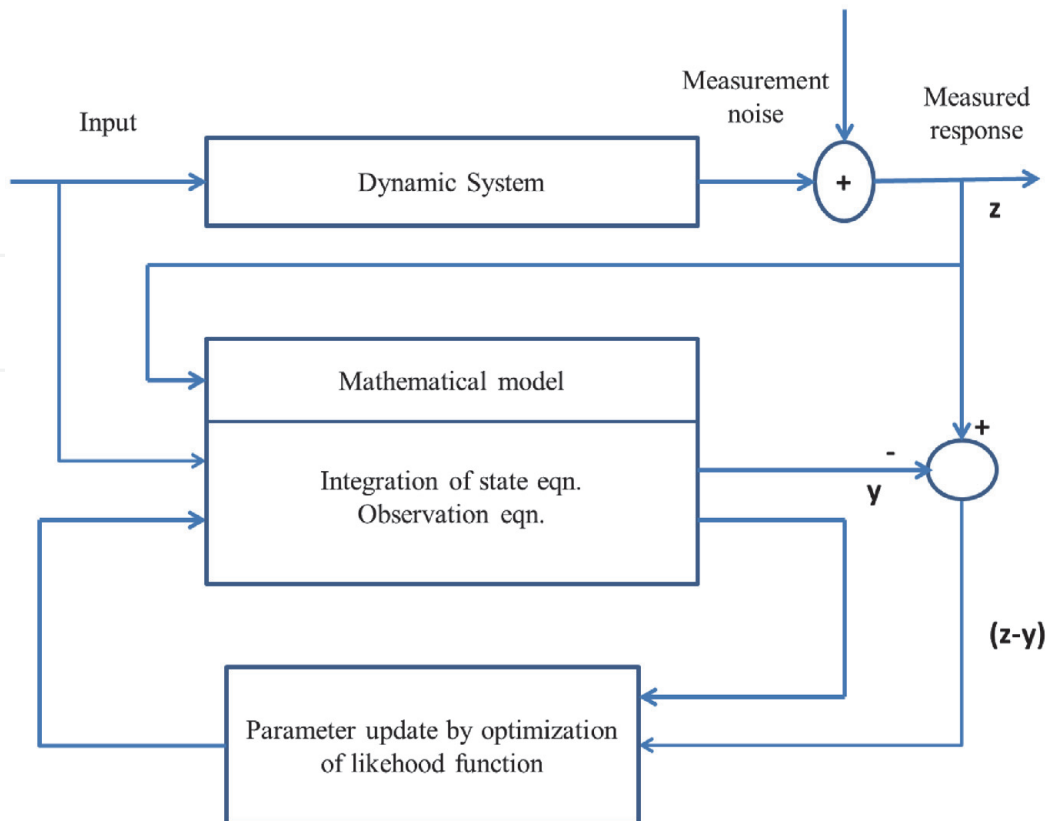


Figure 13.
Block schematic of the output error method.

Give the initial value of the Θ , i.e. Θ_0 . It may also consist of initial value of states x_0 if not known and biases in measurements Δz if required.

Step 1: Set iteration = 1.

Step 2: Compute the response and cost function J :

$$\begin{aligned} \dot{x}(t) &= Ax(t) + Bu(t) \\ y(t) &= Cx(t) + Du(t) \\ R &= \frac{1}{N} \sum_{k=1}^N [z(t_k) - y(t_k)]^T [z(t_k) - y(t_k)] \\ J &= \frac{1}{2} \sum_{k=1}^N [z(t_k) - y(t_k)]^T R^{-1} [z(t_k) - y(t_k)] + \frac{N}{2} \ln |R| \end{aligned} \quad (36)$$

Step 3: Perturb the parameter j , i.e., Θ_j to $\Theta_j + \Delta\Theta_j$, so that system matrices becomes $A_p B_p C_p D_p$.

Step 4: Compute the perturbation responses and update on Θ .

$$\begin{cases} \dot{x}_p(t) = A_p x_p(t) + B_p u(t) \\ y_p(t) = C_p x_p(t) + D_p u(t) \\ \frac{\partial y(t)}{\partial \Theta_j} = \frac{[y_p(t) - y(t)]}{\Delta \Theta_j} \\ \Delta_{\Theta} J(\Theta) = \sum_{k=1}^N \left[\frac{\partial y(t_k)}{\partial \Theta_j} \right]^T R^{-1} [z(t_k) - y(t_k)] \\ \Delta_{\Theta}^2 J(\Theta) = \sum_{k=1}^N \left[\frac{\partial y(t_k)}{\partial \Theta_j} \right]^T R^{-1} \left[\frac{\partial y(t_k)}{\partial \Theta_j} \right] \\ \Theta = \Theta + [\Delta_{\Theta}^2 J(\Theta)]^{-1} [\Delta_{\Theta} J(\Theta)] \end{cases} \quad (37)$$


Step 5: Increment the iteration count and jump back to step 2 to continue until the cost function reduces to zero approximately. Thus estimated parameter Θ is the updated at which cost function is minimized.

Author details

Majeed Mohamed
 CSIR-National Aerospace Laboratories, Bangalore, India

*Address all correspondence to: majeed_md_123@rediffmail.com

IntechOpen

© 2021 The Author(s). Licensee IntechOpen. This chapter is distributed under the terms of the Creative Commons Attribution License (<http://creativecommons.org/licenses/by/3.0>), which permits unrestricted use, distribution, and reproduction in any medium, provided the original work is properly cited. 

References

- [1] Petersen, C., M. Mühleisen, and A. Timm-Giel. Modeling aeronautical data traffic demand. in *Wireless Days (WD)*. 2016, March. IEEE.
- [2] Habibullah, M. and M. Ahsanullah, "Estimation of parameters of a Pareto distribution by generalized order statistics," *Communications in Statistics-Theory and Methods*. 29, no. 7 (2000): 1597–1609,
- [3] Yifei, Z., et al. "Method to analyze air traffic situation based on air traffic complexity map," Paper presented at 9th USA/Europe Air Traffic Management Research and Development Seminar (ATMf2011), Berlin, June, 2011.
- [4] Basu, A., et al., "Geometric algorithms for optimal airspace design and air traffic controller workload balancing," *Journal of Experimental Algorithmics (JEA)*. 14, (2010): 2–3,
- [5] Irvine, D., et al., "A Monte-Carlo approach to estimating the effects of selected airport capacity options in London," *Journal of Air Transport Management*. 42, no.1–9 (2015),
- [6] Leiden, K., P. Kopardekar, and S. Green. "Controller workload analysis methodology to predict increases in airspace capacity," Paper presented at AIAA's 3rd Annual Aviation Technology, Integration, and Operations (ATIO) Forum, 2003.
- [7] Hopkin, V.D., *Human factors in air traffic control*. (London: (Taylor & Francis, 1995).
- [8] Majumdar, A. "The crisis in European air traffic control: An assessment of controller workload modeling techniques," Paper presented at, 1996, Taylor & Francis Ltd.
- [9] Majumdar, A. and W.Y. Ochieng, *A Review of Airspace Capacity and Controller Workload Report to Eurocontrol*. 2000: Contract No. C/1.108/H0/GC/99.
- [10] Subotic, B., W. Ochieng, and A. Majumdar, "Equipment failures in ATC: Finding an appropriate safety target," *Aeronautical Journal*. 109, (2005): 277–284, 10.1017/S0001924000000737.
- [11] SIMMOD Simulation Airfield and Airspace Simulation Report, Oakland International Airport. 2006, ATAC Corporation.
- [12] Hopkin, V.D., *Human factors in air traffic control*. (CRC Press, 2017).
- [13] Hart, S.G.a.S., L.E., *Development of the NASA-TLX (Task Load Index): Results of empirical and theoretical research*, in *Human Mental Workload*. 1988: North-Holland.
- [14] Wickens, C.D., et al., *Engineering psychology and human performance..* 2015: Psychology Press.
- [15] EUROCONTROL, AMS (Air Traffic Control Model Simulation Studies) - an introduction for potential users, in *Internal EEC Note No. 2/AMS/1996, Model Based Simulations Sub-Division*. 1996, EUROCONTROL: France.
- [16] Magill, S.A.N. "Trajectory predictability and frequency of conflict-avoiding action," Paper presented at CEAS 10th International Aerospace Conference, Amsterdam, Netherlands, 1997.
- [17] Welch, J.D., Andrews, J. W., Martin, B. D., and Sridhar, B., . "Macroscopic Workload Model for Estimating En Route Sector Capacity," Paper presented at *Proceedings of the 7th ATM Seminar*, Barcelona, Spain, July 2007.
- [18] Majumdar, A., Ochieng, W. Y., McAuley, G., Lenzi, J. M., and Lepadatu,

C.,” The Use of Panel Data Analysis Techniques in Airspace Capacity Estimation,” *Air Traffic Control Quarterly*. 14, no.1 (2006): 95–115.

[19] Welch, J.D., Andrews, J. W., Martin, B. D., and Shank, E. M.,” Applications of a Macroscopic Model for En Route Sector Capacity,” Paper presented at Proceedings of the AIAA Guidance, Navigation, and Control Conference, AIAA, Honolulu, Hawaii, August 2008.

[20] FAA. Order JO 7210.3 W facility operation and administration (2010), Report, U.S Department of Transportation.

[21] Mitchell, J.S.B., Polishchuk, V., and Krozel, J.” Airspace Throughput Analysis Considering Stochastic Weather,” Paper presented at Proceedings of the AIAA Guidance, Navigation, and Control Conference, Keystone, CO, August 2006.

[22] Krozel, J., Mitchell, J. S. B., Polishchuk, V., and Prete, J.” Capacity Estimation for Airspaces with Convective Weather Constraints,” Paper presented at Proceedings of the AIAA Guidance, Navigation, and Control Conference, Hilton Head, SC, H, August 2007.

[23] Zou, J., Krozel, J. W., Krozel, J., and Mitchell, J. S. B.” Two Methods for Computing Directional Capacity given Convective Weather Constraints,” Paper presented at Proceedings of the AIAA Guidance, Navigation, and Control Conference, Chicago, IL, August 2009.

[24] Zhang, M., et al.,” Terminal airspace sector capacity estimation method based on the ATC dynamical model,” *kybernetes*. 45, (2016): 884–899, doi.org/10.1108/K-12-2014-0308.

[25] Bence Szamel., I.M., and Geza Szabo,” Applying Airspace Capacity

Estimation Models to the Airspace of Hungary,” *Periodica Polytechnica Transportation Engineering*. 43, no.3 (2015): 120–128, doi.org/10.3311/PPtr.7512.

[26] Mohamed, M. and V. Dongare, Aircraft Aerodynamic Parameter Estimation from Flight Data Using Neural Partial Differentiation. 1st ed. Springer; 2021. DOI:10.1007/978-981-16-0104-0

[27] Laudeman, I.V., et al., Dynamic Density: An Air Traffic Management Metric. NASA-TM-1998-112226, April 1998.

[28] Maine, R. E. and Iliff, K. W. Identification of Dynamic Systems - Applications to Aircraft Part 1: The Output Error Approach AGARD, AG-300, 1986, 3.

[29] Majeed, M. and Kar, I. N. Identification of aerodynamic derivatives of a flexible aircraft using output error method *Applied Mechanics and Material, Mechanical and Aerospace Engineering*, 2012, 110–116, 5328–5335.

[30] Mehra, R.; Stepner, D. and Tyler, J. Maximum likelihood identification of aircraft stability and control derivatives *Journal of aircraft*, 1974, 11, 81–89.